SAND2011-1527C

Power Handling and Intermodulation Distortion of Contour-Mode AlN MEMS Resonators and Filters

Christopher D. Nordquist and Roy H. Olsson III

Sandia National Laboratories, Albuquerque, NM 87185, USA

***Abstract* — We report measurements of the power handling and intermodulation distortion of piezoelectric contour mode resonators and filters operating near 500 MHz. The output power capability scales as the inverse of the motional impedance squared, and the power handling of resonator filter circuits scales with the number of resonators combined in series and parallel. Also, the third-order intercept depends on the measurement tone spacing. Individual AlN resonators with 50 Ω motional impedance demonstrate output power capability of +10 dBm and OIP_3 > +20 dBm, while an eight resonator filter demonstrates output power handling of +14 dBm and a OIP_3 > +32 dBm.**

***Index Terms* — Resonator Filters, piezoelectric devices, intermodulation distortion, radiofrequency microelectromechanical systems.**

I. Introduction

Contour-mode piezoelectric resonators offer high Q and low device impedance. These attributes, coupled with the use of lithographic dimensions to determine the resonant frequency of the device, make these devices ideal for miniature integrated filter banks [1]. In addition to insertion loss and bandwidth, two key attributes for band select and channel select filters are power handling and intermodulation distortion. In order for these filters to be practical for many RF front-end filter applications, these properties must be characterized and understood.

The intermodulation distortion of a device is commonly described by the third-order intermodulation product (IP_3), which is the power level point where the extrapolated power of close-in third-order intermodulation products equals that of the two carrier tones [2]. In cases where both the power handling and intermodulation distortion are determined by the same nonlinear processes, the IP_3 is generally 9 dB higher than the 1 dB compression point (P_{1dB}) of the same device.

In this work, we report initial power handling and intermodulation characterization of AlN contour-mode MEMS resonators. While intermodulation and power handling has been reported for other types of piezoelectric resonator-based filters such as bulk acoustic wave resonators [3] and surface acoustic wave resonators [4], the power handling and intermodulation of contour mode resonators and filters has not been studied aside from limited conference reports [5,6].

In this paper, we report the power handling and intermodulation performance of MEMS AlN resonators as a function of impedance and tone separation. Additionally, we compare the intermodulation performance of an individual device to that of a filter synthesized from microresonators.

II. Experimental

The MEMS resonators and filters measured in this work were fabricated using processes similar to those described previously [7]. In this work, measurements were taken from two different wafers, described as "A" and "B", which were fabricated in separate lots with different masksets. Aside from minor changes such as the center frequency, the resonator designs were unchanged between the two masksets. The resonators and filters were designed and fabricated with nominal center frequencies of 500 MHz and motional impedances of approximately 50 Ω.

An example contour-mode microresonator is shown in Fig. 1. The active region of the resonator is defined by the interdigitated fingers that are on top of a freestanding film of AlN. The fingers are separated on a pitch of one half of the acoustic wavelength at the resonant frequency. Additionally, the total width of the AlN bridge perpendicular to the fingers is designed to be a multiple of one half wavelength at resonance. For a 500 MHz resonator, the finger pitch is approximately 9 µm. The motional impedance of the resonator is determined by the overall size of the device, and can be changed by varying either the number of fingers in the device or the length of the device fingers. For the eight 320 µm-long fingers shown in Fig. 1, the device motional impedance is approximately 60 Ω.

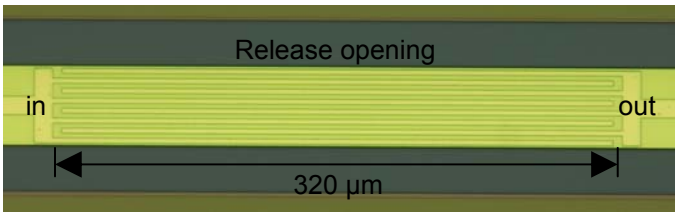

Fig. 1: Optical micrograph of a single AlN MEMS resonator with eight 320 µm-long interdigitated fingers on a suspended AlN membrane.

The measurements described in this paper were taken using a Maury Automated Test System [8] coupled with a Cascade Microtech Probe Station. The system was calibrated at the GSG150 probe tips using the LRRM method with the tuners set to the Z_o position for all measurements. The two tones for

the intermodulation measurements were generated by HP8340 synthesized sweepers that were amplified by a two-channel amplifier. Each tone passed through an isolator before combining. The carrier and intermodulation products were measured using an HP8562A spectrum analyzer and the total output power was measured using an Agilent E4419B power meter. Prior to and following the power sweeps, s-parameters were measured using an Agilent E9364B PNA.

III. Intermodulation of Single Resonators

Two resonators with different device impedances from wafer A were tested at their center resonant frequencies. The resonators each had 7 fingers on a 9 µm pitch, with finger lengths of 520 µm for the 50 Ω resonator and 260 µm for the 100 Ω resonator. The small-signal insertion loss, measured at an input power of 0 dBm, of these two resonators is shown in Fig. 2. The 50 Ω resonator has a minimum 3.8 dB insertion loss at 488.2 MHz, while the 100 Ω resonator has a minimum of 6.6 dB insertion loss at 487.0 MHz. In both cases, the loaded Q of the resonator is greater than 300.

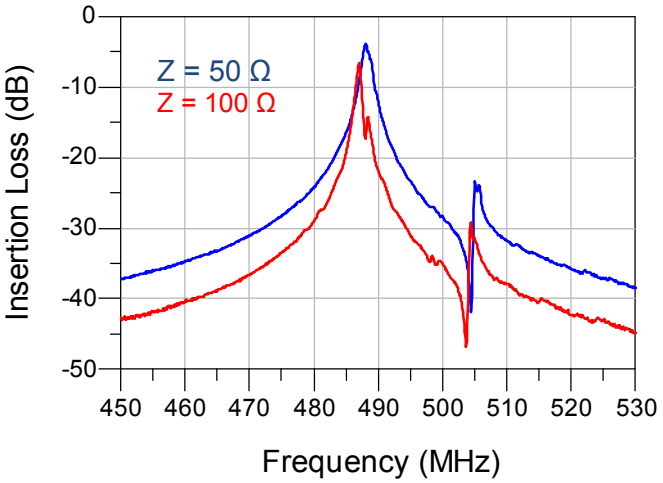

Fig. 2: Small signal insertion loss of the 50 Ω and 100 Ω resonators tested from wafer A.

The intermodulation of the two resonators was tested with two tones centered at the center frequency of the resonator and separated by 100 kHz. The magnitude of the output carrier and third-order products as a function of total input power is plotted in Fig. 3 for the two different resonators. The plot includes extrapolations of the fundamental and third-order power levels in order to extrapolate a third order intercept value. Note that the total output power is 3 dB higher than the carrier value because each carrier tone contains half of the total output power.

Because of the lower loss, the 50 Ω resonator has a higher output power at a given input power. The insertion loss of the resonator degrades gradually by 1-2 dB as the input power is increased from -20 dBm to +10 dBm, and then degrades rapidly when the maximum power handling of the resonator is exceeded. The initial degradation in insertion loss is typically recoverable, while the sudden degradation is generally permanent, corresponding to device damage. The 50 Ω resonator exhibits this rapid gain compression above an input power of 18 dBm and an output power of 10 dBm, while the 100 Ω resonator demonstrates rapid compression beyond an input power of 15 dBm and an output power of 4 dBm. Thus, the output power handling of the resonator scales by the inverse square of the impedance because both the input power handling and the insertion loss of the resonator scale as the inverse of the impedance and device area.

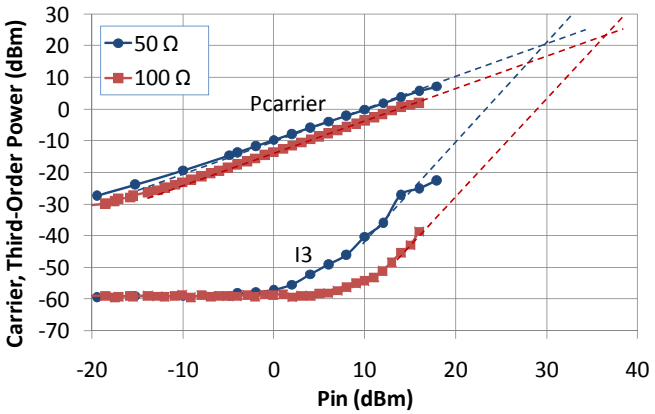

Fig. 3: Carrier power (Pcarrier) and third-order intermodulation products (I3) for the 50 Ω and 100 Ω resonators. The test tones are separated by 100 kHz and centered at the frequency of minimum loss for each resonator (487 MHz for the 100 Ω device and 488.2 MHz for the 50 Ω device).

The third-order intercept of each resonator was extrapolated using two different approaches. The first method was performed at each power level by calculating the third order intercept using the difference between the power levels in the fundamental and intermodulation tones. The second method, shown in Fig. 3, used an extrapolation of the fundamental tone power with a slope of 1:1 and the third-order intermodulation power with a slope of 3:1. Using either method, the output-referred third order intercept for each device was approximately +20 dBm. It is not clear why the IP3 is similar for both devices, or if this relationship will hold for other differences in impedance, but the ~10 dB difference between the compression point and the third-order intercept is consistent with the expected behavior for an individual device measured with two in-band tones.

IV. Series and Filter Connected Resonators

A primary application of these MEMS resonators is the realization of ladder and other filters, where multiple resonators are used to synthesize a specific band shape response. To investigate this, the intermodulation response of a single resonator and two other filters were evaluated.

The measured single resonator had eight 320 µm-long fingers on a 9 pitch, had a nominal motional impedance of 60 Ω, and was identical to the one shown in Fig. 1. The

two filters were synthesized by the series connection of two banks of these resonators to increase the out-of-band rejection. In the case referred to as the 1 x 2 filter, the filter was realized with a series combination of two single resonators. In the other case, referred to as the 4 x 2 filter, the filter was realized by using a series combination of two parallel arrays of four resonators each, as shown in Fig. 4.

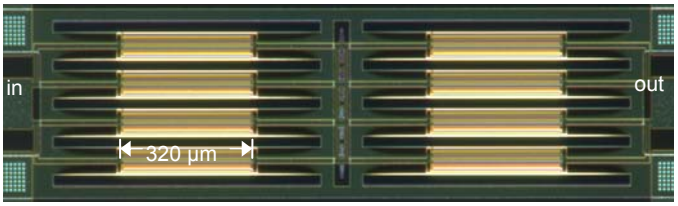

Fig. 4. Optical image of a 4 x 2 MEMS resonator filter realized by the series combination of two banks of four parallel 60 Ω resonators each.

The small signal s-parameter response of both the individual resonator and the filters in Fig. 5 shows the improved rejection obtained by the series connection of the resonators and the wider bandwidth obtained by the series-parallel combination of the resonators. While actual the center frequencies vary slightly from 500 MHz, the filter responses have been normalized to 500 MHz for ease of comparison.

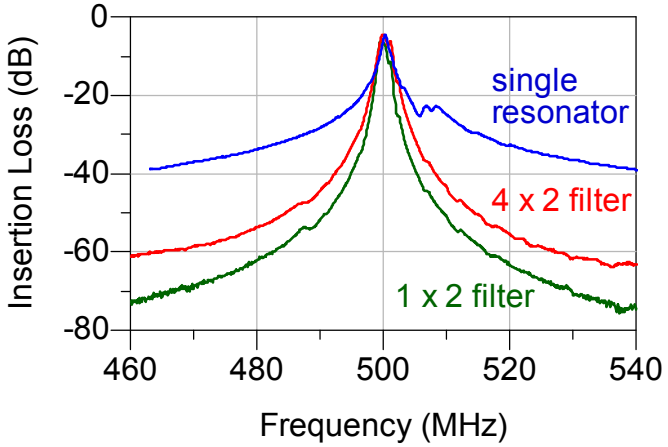

Fig. 5. Small-signal s-parameter response of the single resonator and filters.

The two-tone measurement results from the individual resonator and the filters are shown in Fig. 6. As in the previous measurement, the two tones are centered around the center frequency of the device with a tone separation of 100 kHz. The insertion losses are similar for all three devices at the center frequency, but the power handling of the individual resonator and the 1 x 2 filter is lower than that of the 4 x 2 filter. The individual resonator begins to demonstrate compression at an input power of +11 dBm and total output power of +5 dBm, the 1 x 2 filter starts to enter compression at an input power of +14 dBm and an output power of +7 dBm, and the 4 x 2 filter enters compression at an input power above +20 dBm and output power above +14 dBm. Thus, it appears that the series combination of two resonators increases the power handling by a factor of two, and the combination of four resonators in parallel increases the power handling by another factor of four. This suggests that the intermodulation mechanism is related to the total power stored in the resonator, rather than the voltage at the input of the first resonator.

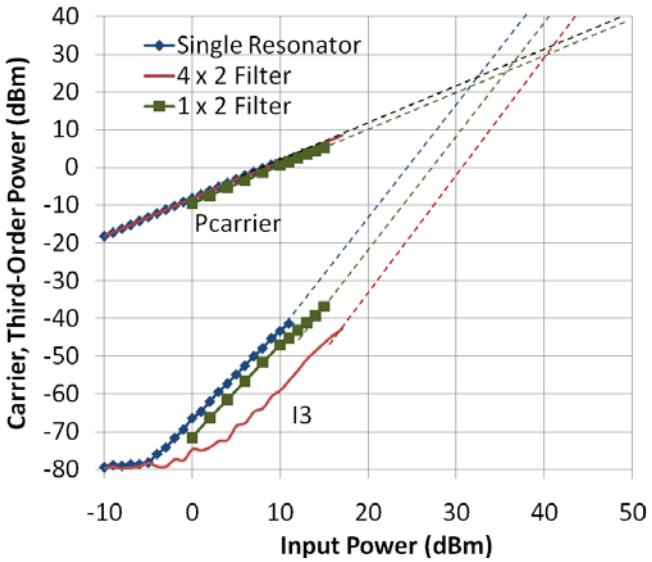

Fig. 6. Carrier power and third-order intermodulation power as a function of input power for a single resonator, a 1 x 2 filter, and a 4 x 2 filter. The measurement frequency is centered at the center frequency of each device and the tone separation is 100 kHz.

Fig. 6 also includes the extrapolation of the carrier tone power and the third-order intermodulation tone power for estimating the filter third-order intercept. The third-order intercepts of the single resonator, 1 x 2 filter, and 4 x 2 filter are +23 dBm, +25 dBm, and +32 dBm, respectively. These values are approximately 18 dB above the output power at which the device began exhibiting gain compression.

V. EFFECT OF TONE SPACING

To evaluate the effect of the tone spacing, the 4 x 2 filter was measured with tone spacings varying from 0.1 MHz to 3 MHz. For a filter with a 3-dB bandwidth of 2 MHz, both the carrier and third-order tones are in-band at narrow frequency spacings, while at frequency spacings between 1 MHz and 2 MHz, the carrier tones are in-band and the third-order tones are out-of-band. At tone spacings above 2 MHz, both the carrier tone and third-order tones are out-of-band.

The filter was tested at a carrier input power of +12 dBm (+15 dBm total power) with the tones centered midway between the two 3 dB points in the filter response. The frequency spacing was swept from 0.1 MHz to 3 MHz in

0.1 MHz steps, corresponding to frequency offset of 0.05 MHz to 1.5 MHz from the filter center frequency.

The output carrier power, third-order intermodulation power, and calculated third-order intercept from this measurement are shown in Fig. 7. The small-signal filter response is also included on the plot for reference. It is important to note that the third-order power is plotted at the offset frequency of the carrier for the measurement; the actual third-order signal is at twice the offset.

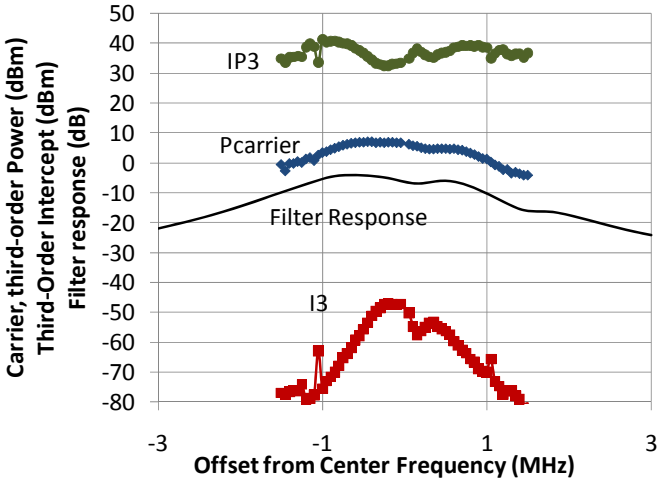

Fig. 7. Carrier power, third-order intermodulation product power, third-order intercept value, and filter response vs. offset from filter center frequency.

As expected, the carrier power tracks the measured insertion loss of the filter closely. The third-order products also appear to track the filter response, but when the offset is 0.5 MHz, the carriers remain in band but the intermodulation products begin to fall out-of-band, lowering the power in the third-order products and increasing the apparent third-order intercept of the filter at this frequency spacing. This apparent increase in third-order intercept increases until the carrier tones also fall out of the filter bandwidth and begin to be attenuated.

VI. CONCLUSIONS

While MEMS resonators offer the potential for miniature integrated filter banks, intermodulation distortion and power handling remain important performance metrics for band select and channel select filters. AlN contour-mode resonators have been characterized for power handling and intermodulation, with individual 50 Ω-impedance resonators demonstrating the ability to handle input powers up to +18 dBm and output powers up to +10 dBm without performance degradation. The input power handling of the resonators scales inversely with impedance, while the output power handling scales inversely as the square of the impedance. Series and parallel combinations of resonators also appear to increase the power handling and third-order intercept of a filter by a factor of the number of resonators, with a filter comprised of eight 60 Ω-impedance resonators demonstrating output power handling of +14 dBm and a third-order intercept of +32 dBm. Finally, the intermodulation performance of an AlN filter varies with tone spacing due to additional attenuation when the intermodulation tones fall outside of the filter bandwidth.

ACKNOWLEDGEMENT

Sandia National Laboratories is a multi program laboratory managed and operated by Sandia Corporation, a wholly owned subsidiary of Lockheed Martin Corporation, for the U.S. Department of Energy's National Nuclear Security Administration under contract DE-AC04-94AL85000. This work was supported by the Laboratory Directed Research and Development Program, and the authors acknowledge management support from K. Ortiz, C. T. Sullivan, and T. E. Zipperian, as well as fabrication support from M. Tuck and the MESAFab operations team.

REFERENCES

[1] C. Zuo and G. Piazza, "Single-Ended-to-Differenetial Channel-Select Filters Based on Piezoelectric AlN Contour-Mode MEMS Resonators, *Proc. 2010 IEEE Freq. Cntl. Symp.*, pp. 5-8, June 2010.

[2] D. Pozar, *Microwave Engineering*, Reading, MA: Addison-Wesley, 1990.

[3] E. Rocas, C. Collado, A. Padilla, J. Mateu, and J. M. O'Callaghan, "Nonlinear distributed model for IMD prediction in BAW resonators," *Proc. 2008 IEEE Intl. Ultrasonics Symp.*, pp. 1557-1560, Nov. 2008.

[4] G. Coussot, "Investigation of Intermodulation in Acoustic-Surface-Wave Filter," *Electronics Lett.*, vol. 11, no. 5, pp. 116-117, March 1975.

[5] C. Zuo, N. Sinha, M. B. Pisani, C. R. Perez, R. Mahameed, and G. Piazza, "Channel-Select RF MEMS Filters Based On Self-Coupled AlN Coupled Contour-Mode Piezeoelectric Resonators," *Proc. 2007 IEEE Intl. Ultrasonics Symp.*, pp. 1156-1159, Oct. 2007.

[6] C. Zuo, M. Rinalsi, and G. Piazza, "Power Handling and Related Frequency Scaling Advantages in Piezoelectric AlN Contour-Mode MEMS Resonators, *Proc. 2009 IEEE Intl. Ultrasonics Symp.*, pp. 1187-1190, Oct. 2009.

[7] R. H. Olsson, III, K. E. Wojciechowski, M. S. Baker, M. R. Tuck, and J. G. Fleming, "Post-CMOS-Compatible Aluminum Nitride Resonant MEMS Accelerometers," *IEEE J. Microelectromech. Sys.*, vol. 18, no. 3, pp, 671-678, June 2009.

[8] Maury Microwave Corporation ATS v. 5.1, http://www.maurymw.com